

New Alkali Doped Pillared Carbon Materials Designed to Achieve Practical Reversible Hydrogen Storage for Transportation

Wei-Qiao Deng, Xin Xu,* and William A. Goddard[†]

Materials and Process Simulation Center, Division of Chemistry and Chemical Engineering, California Institute of Technology, Pasadena, California 91125, USA

(Received 29 May 2003; published 21 April 2004)

We propose a new generation of materials to maximize reversible H₂ storage at room temperature and modest pressures (< 20 bars). We test these materials using grand canonical Monte Carlo simulations with a first-principles-derived force field and find that the Li pillared graphene sheet system can take up 6.5 mass% of H₂ (a density of 62.9 kg/m³ at 20 bars and room temperature. This satisfies the DOE (Department of Energy) target of hydrogen-storage materials for transportation. We also suggest ways to synthesize these systems. In addition we show that Li-doped pillared single-wall nanotubes can lead to a hydrogen-storage capacity of 6.0 mass% and 61.7 kg/m³ at 50 bars and room temperature storage, which is close to the DOE target.

DOI: 10.1103/PhysRevLett.92.166103

PACS numbers: 68.43.-h, 61.46.+w

Perhaps the most promising technology to dramatically decrease pollution while conserving the decreasing supply of fossil fuel is the use of hydrogen fuel cells in transportation. Unfortunately this solution is impeded by the lack of safe and economical ways to store the hydrogen on board a vehicle. The U.S. Department of Energy (DOE) has estimated that attaining a suitable driving range for automotive applications will require storing 6.5 mass% of hydrogen (density of 62.5 kg/m³), whereas the best materials such as cubic TiV₂ can storage only up to 2.6 mass% at 10 bars and 313 K [1].

Recent claims of large hydrogen uptake for lightweight nanostructured carbon materials, in the form of tubes [2–5], fibers [6,7], and mechanically milled graphite [8], have attracted considerable experimental and theoretical interest. For example, Ye *et al.* used high-purity single-walled carbon nanotubes (SWNTs) and obtained ~8.0 mass% of H₂ adsorption at 80 K and above 100 bars [3]. Browning *et al.* reported that 6.5 mass% hydrogen can be stored in carbon nanofibers under conditions of 120 bars pressure and ambient temperature [7]. These H₂ uptake systems require either high pressure [7] or very low temperature [6] or both [3] that limit the applicability for mobile applications that require working conditions of roughly 1–20 bars and ambient temperature. Chen *et al.* reported remarkable hydrogen-storage capacities of 20 mass% for Li-doped nanotubes at 653 K and 14 mass% for K-doped nanotubes at room temperature [9]. They also reported smaller but still significant absorptions in alkali doped graphite (14 mass% for Li and 5 mass% for K) [9]. Unfortunately, later studies revealed that these high H₂ uptakes were due to the impurity water gain/loss present in the hydrogen feedstream rather than to H₂ itself [10,11].

We report here a new class of materials for reversible hydrogen storage designed to meet the criteria for transportation applications. To validate our design we use a

multiscale computational strategy [12,13], in which quantum mechanics (QM) at the X3LYP [14] level of density functional theory (DFT) developed to accurately treat van der Waals interactions is used to determine an accurate force field (FF) [15]. We then use this FF with grand canonical Monte Carlo (GCMC) simulations to determine the H₂ uptake as a function of pressure and temperature [13].

As discussed below, normal condensed graphite and nanotube systems are too dense to bind sufficient H₂ and we also considered graphene sheet and SWNT systems pillared to provide more space. To determine the optimum performance, we first ignore the space taken by the pillars and then address it later. For our model SWNT we consider (10,10) which leads to a tube diameter of ~13.6 Å, close to the mean diameter most frequently observed in SWNT synthesized by the arc-discharge or pulsed-laser vaporization techniques [16]. Curves (a)–(c) in Fig. 1(b) show the predicted H₂ storage at 300 K and

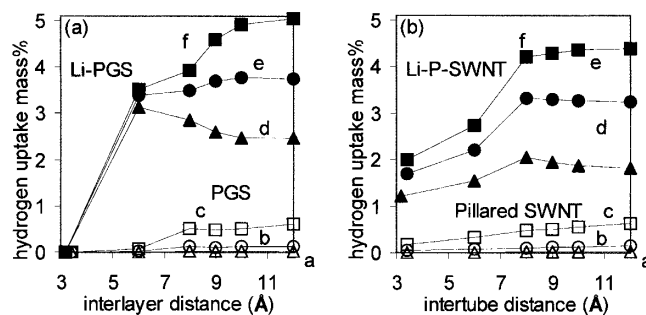


FIG. 1. Dependence of the mass hydrogen storage capacity on the interlayer (intertube) distances under various pressures for (a) PGS (white) and Li-GIC or Li-PGS (black); and (b) (10,10) SWNTs (white) and Li-P-SWNT (black) systems. The doping concentration is Li:C = 1:6. The pressures are square = 50 bars; circle = 10 bars, and triangle = 1 bar.

various pressures for pure pillared SWNTs (P-SWNT) as a function of the intertube distance (ITD) between the SWNT. The first point at 3.4 Å corresponds to the equilibrium ITD in the SWNT crystal, where we find 0.2 mass% at 50 bars, due entirely to the internal spaces of the SWNTs. These results are in good agreement with recent experiments [2,3,6] and computations on SWNTs [17]. Thus Ye *et al.* [3,6] reported 2–4 mass% storage for 20–50 bars at 80 K, comparable to our calculated results of 3–4 mass% at the same conditions; Hirscher [2] reported 0.005 mass% storage at 300 K and 1 bar while we calculate 0.01 mass% under these conditions. For P-SWNT we find a slight increase to 0.1 mass% at 10 bars and 0.5 mass% at 50 bars for ITD > 8 Å. The performance of pure pillared graphene sheets (PGS) is similar. Curves (a)–(c) in Fig. 1(a) show the predicted hydrogen storage for a function of the interlayer distance (ILD). The first point (3.4 Å) corresponds to the equilibrium ILD in bulk graphite, leading to zero hydrogen uptake. As the ILD is increased to over 8 Å, we find that the hydrogen uptake for PGS reaches 0.1 mass% at 10 bars and 0.5 mass% at 50 bars. Thus we conclude that the hydrogen-storage capacity at ambient conditions is very limited for carbon-only systems such as graphene sheets and SWNTs, even if pillared to provide more space for the hydrogen.

In order to increase the hydrogen-storage capacity, we considered adding Li to the PGS and P-SWNT systems. Our reasoning was that the high electron affinity of the sp^2 carbon framework would separate the charge from the Li, providing strong stabilization of the molecular H_2 . We first considered a Li-doping concentration of Li:C = 1:6, which corresponds to the most stable conformation of Li-GIC (graphite intercalated compound) at ambient conditions. Curves (d)–(f) in Fig. 1(a) show the results for Li-PGS. The first point at ILD = 3.4 Å shows that Li-GIC does *not* exhibit hydrogen-storage capacity, in agreement with the experimental observation of Pinkerton *et al.* [11]. Curves (d)–(f) in Fig. 1(b) show the results for Li-P-SWNT. The equilibrium ITD of 3.4 Å leads to 1.2 mass% hydrogen storage at 1 bar, which increases to ~2.0 mass% for 50 bars. Here 99.5% of the storage comes from the space *inside* the nanotubes. These results suggest an explanation for the differences observed between different experiments [10]. Pinkerton [11] found no observable hydrogen-storage capacity for Li-doped nanotubes, but they used closed-end nanotubes that would prevent H_2 from entering the tubes. Yang [10] made nanotubes by chemical vapor deposition followed by purification with strong acid, which will cut off the nanotube caps [10], allowing the H_2 to go inside. The found ~2.5 mass% hydrogen storage for Li-doped nanotubes at 1 bar and ambient temperature. This is consistent with our results of 1.2 mass% at the same conditions. The small discordance here might be because we considered the infinite crystal with no surfaces, whereas the experiments probably had

substantial surface area which might increase the net storage. We conclude that Li-doped carbon SWNTs do exhibit modest hydrogen-storage capacity at ambient conditions, but not enough to meet the DOE requirements for transportation. Consequently we will explore below how the hydrogen storage can be increased with additional Li-doping and modified nanostructures. The results in Fig. 1 show that a Li-PGS and Li-P-SWNT in which graphene or SWNT sheets are separated by ILD or ITD of 6 to 12 Å significantly enhance the storage capacity. This is in sharp contrast to the situation for undoped PGS or P-SWNTs where increasing the ILD or ITD has a very limited effect on the storage capacity. This is also in contrast to the un-pillared system where Li doping has only a very modest effect on hydrogen storage. The Li-doped pillared systems also lead to a much larger benefit from increased pressure. Thus Fig. 1 shows that at 10 bars and room temperature the hydrogen-storage capacity increases from 0.1 mass% for PGS to 3.7 mass% for Li-PGS (Li:C = 1:6) with the ILD increased to 10 Å.

Our simulations show that Li dopants act as positive (acidic) cores that attract hydrogen molecules. The lack of hydrogen-storage capacity in ordinary graphite and SWNT systems is due to the restricted space available around the Li dopants. These results suggest that by pillaring to increase the interlayer distances and by increasing the Li-doping concentration, it may be possible to reach the DOE goal with Li-doped pillared carbon-based materials.

Given the very favorable synergetic affect of combining Li doping with pillaring of graphitic sheets, we considered optimizing the amount of Li. Figure 2(a) shows that increasing the Li-doping concentration increases the hydrogen-storage capacity nearly linearly, increasing from 3.7 mass% at Li:C = 1:6 to 6.5 mass% at Li:C = 1:3 (for Li-PGS with ILD = 10 Å at 10 bars). To determine the maximum feasible concentration, we carried out a DFT

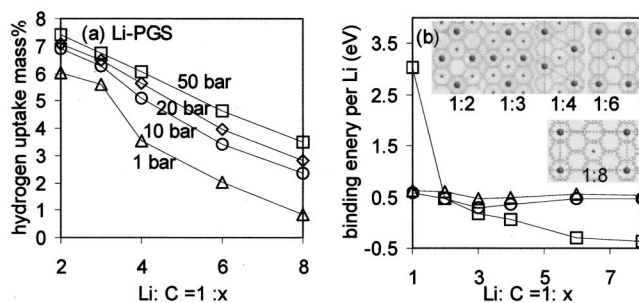


FIG. 2. (a) Effects of Li-doping concentration on the mass hydrogen storage capacity under various pressures. ILD = 10 Å. (b) Binding energy per Li atom under various Li-doping concentrations. Keys in (b) square = equilibrium interlayer distance; circle = interlayer distance 8 Å; triangle = interlayer distance 10 Å. The zero energy reference responds to pure graphite crystal and pure Li metal.

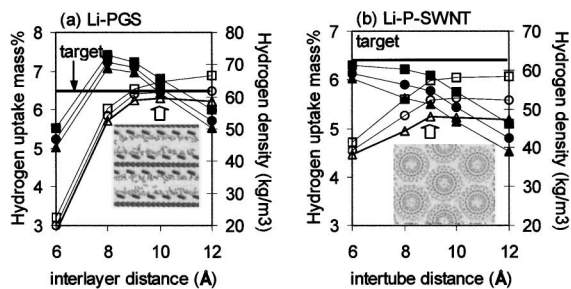


FIG. 3. Optimization of nanostructures of (a) Li-PGS and (b) Li-P-SWNT systems for mass (white) and volumetric (black) hydrogen storage capacities. The Li-doping concentrations are Li:C = 1:3. The DOE target is shown by a line. The optimum interlayer or intertube distance is indicated by an arrow. Key: square = 50 bars; circle = 20 bars, and triangle = 10 bars.

calculation on Li-GIC and Li-PGS for various Li:C ratios [18]. Figure 2(b) shows that at the equilibrium interlayer distance Li-GIC is most stable for Li:C = 1:6 and Li:C = 1:8, in agreement with experimental observation. However, for Li-PGS, Li:C = 1:3 is the most stable structure for $ILD > 8 \text{ \AA}$. Figure 3(a) shows the hydrogen-storage performance for the optimum Li-PGS (Li:C = 1:3 and $ILD = 10 \text{ \AA}$). At room temperature and 20 bars this leads to hydrogen storage of 6.5 mass% and 62.9 kg/m^3 , which fulfills the DOE requirements (6.5 mass% and 62 kg/m^3). The DOE target could be surpassed to 6.7 mass% and 65.8 kg/m^3 with an operating pressure of 50 bars. Figure 3(b) shows the results for Li-P-SWNT for Li:C = 1:3 and $ITD = 9 \text{ \AA}$. Here we find hydrogen storage of 6.0 mass% and 61.7 kg/m^3 at room temperature and 50 bars. Thus Li-PGS has better hydrogen-storage performance than Li-P-SWNT and is likely to be much less expensive, making Li-PGS an excellent candidate for developing a practical H_2 storage system for transportation. Figure 4 illustrates how temperature and pressure effects can be used to design the load/unload operating process for a reversible hydrogen-storage system. For example Li-PGS (Li:C = 1:3 with $ILD = 10 \text{ \AA}$) reaches 6.5 mass% hydrogen uptake under loading conditions of 20 bars and 300 K. Under the unloading conditions of 0.01 bar and 400 K, the residual hydrogen is 0.2 mass%. Therefore, the total load/unload will provide 6.3 mass% reversible hydrogen. This is far superior to any other hydrogen-storage system.

Ball milling has been established to effectively increase the Li-doping concentration and is ready to extend to industrial scales [19]. There is also experimental evidence that the ILD of GIC can be expanded. It was proved that either type organic ligands can bind to alkali metal ions and cointercalate into the host carbons so that the interlayer distance of GIC can be expanded from around 3.4 \AA to $8.7\text{--}12.4 \text{ \AA}$ [20]. We believe that the same cointercalation synthesis method can be extended to SWNT

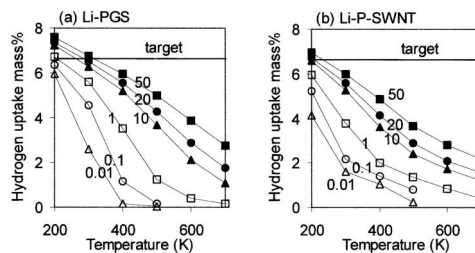


FIG. 4. Temperature and pressure (unit: bar) effects on the mass hydrogen storage capacity. (a) Li-PGS: Li:C = 1:3 and $ILD = 10 \text{ \AA}$; (b) Li-P-SWNT: Li:C = 1:3 and $ITD = 9 \text{ \AA}$.

systems to expand the intertube distances. Figure 5 proposes a possible scheme to synthesize a practical hydrogen-storage system such as the following:

- (i) Ternary compounds are first produced by the reaction between host carbons and 2,5-dihydrofuran solvated Li cation in low concentration such that the interlayer spaces of graphite are expanded.
- (ii) A Diels-Alder-type reaction between the organic solvents and the graphite sheets is triggered to build covalent bonds that would maintain the interlayer space under operating conditions.
- (iii) Li-intercalation and proper ball milling are used to synthesize PGS of higher Li concentration.

We have tested this process with computer simulations. For Li:C = 1:3, we considered one pillar per 116 carbons and find $ILD = 8.0 \text{ \AA}$. Carrying out GCMC calculations on this system we find 5.7 mass% hydrogen storage at 300 K and 50 bars. For maximum performance the pillar should be modified to yield $ILD = 10 \text{ \AA}$.

Summarizing, we have designed a series of new materials for H_2 storage: Li-PGS and Li-P-SWNT. We have tested and optimized the nanostructure of these Li-doped

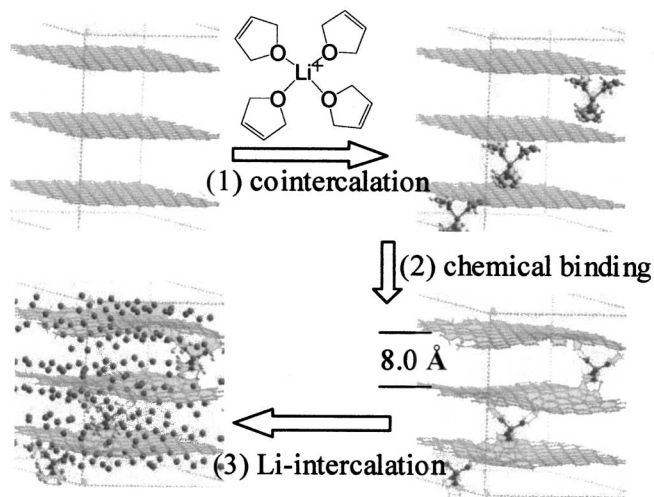


FIG. 5. A scheme to synthesize the Li-doped pillared graphene or nanotubes of high Li-doping concentrations and large interlayer distances.

carbon materials using grand canonical Monte Carlo simulations with a first principles-derived force field. We predict that for 1:3 Li:C doping and $ILD = 10 \text{ \AA}$, Li-PGS will lead to hydrogen storage of 6.5 mass% and 62.9 kg/m^3 at 20 bars and room temperature, attaining the DOE target. We find that Li-P-SWNT (1:3 Li:C doping and $ITD = 9 \text{ \AA}$), can lead to a hydrogen-storage capacity of 6.0 mass% and 61.7 kg/m^3 at 50 bars and room temperature storage, which is close to the DOE target. We also suggest ways to synthesize these systems by cointercalation of solvated Li ion followed by Li-intercalation and ball milling.

This work was supported by the General Motors Corporation (Dr. Gerald Voecks). The facilities of the Materials and Process Simulation Center (MSC) used in these studies were funded by DURIP (ARO and ONR), NSF (CTS and MRI), and a SUR grant from IBM. In addition, the MSC is funded by grants from ARO-MURI, NIH, ChevronTexaco, General Motors, Seiko-Epson, the Beckman Institute, Asahi Kasei, and the Toray Corporation.

*On sabbatical leave from Xiamen University, Xiamen 361005, China.

†To whom correspondence should be addressed.

Email address: wag@wag.caltech.edu

- [1] L. Schlapbach and Z. Zuttel, *Nature (London)* **414**, 353 (2001), and references therein.
- [2] M. Hirscher *et al.*, *Appl. Phys. A-MATER* **72**, 129 (2001).
- [3] Y. Ye *et al.*, *Appl. Phys. Lett.* **74**, 2307 (1999).
- [4] A. C. Dillon *et al.*, *Nature (London)* **386**, 377 (1997); A. C. Dillon *et al.*, in *Proceedings of the 2000 Hydrogen Program Review* (NREL Report No. NREL/CP-507-28890, 2000).
- [5] C. Liu *et al.*, *Science* **286**, 1127 (1999); H. M. Cheng *et al.*, *Z. Metallkd.* **91**, 306 (2000).
- [6] C. C. Ahn *et al.*, *Appl. Phys. Lett.* **73**, 3378 (1998); Y. Y. Fan *et al.*, *Carbon* **37**, 1649 (1999).
- [7] D. J. Browning *et al.*, *Nano Lett.* **2**, 201 (2002).
- [8] S. Orimo *et al.*, *Appl. Phys. Lett.* **75**, 3093 (1999).
- [9] P. Chen *et al.*, *Science* **285**, 91 (1999).
- [10] R. T. Yang, *Carbon* **38**, 623 (2000).
- [11] F. E. Pinkerton *et al.*, *J. Phys. Chem. B* **104**, 9460 (2000).
- [12] To describe the van der Waals (vdW) interactions between the Li dopants, carbon materials, and hydrogen systems we use Morse potentials with the parameters determined by fitting to accurate *ab initio* calculations as described here. (i) For the H-H vdW term, we fitted the potential curve between two H_2 molecules using CCSD(T) *ab initio* QM with the aug-cc-pVQZ basis set. (ii) For the C-H vdW term, we calculated the interaction between H_2 and C_2 molecules using the MP4 *ab initio* QM with the aug-cc-pVTZ basis set plus midpoint bond functions. (iii) To determine the interactions between doped Li ions and hydrogen molecules, we considered a planar C_{32} cluster (ten aromatic rings) doped with one Li atom on each side (in the optimum configuration found for Li:C = 1:3 Li-PGS) to which one H_2 was bonded. These calculations used X3LYP [6-311G(d,p) basis set], a new DFT functional which leads to an accurate description of van der Waals and hydrogen bond interactions [14]. High quality *ab initio* calculations [MP4/6-311G(d,P)//MP2/6-311G(d,p)] have previously been reported [21] showing that Li cation binds six H_2 molecules at zero Kelvin with the enthalpy for adding successive H_2 of -5.39 , -4.3 , -4.07 , -3.65 , -1.87 , and -2.3 kcal/mol; this agrees well with the X3LYP results of -5.12 , -4.47 , -3.9 , -3.63 , -1.55 , and -1.52 kcal/mol for the same system.
- [13] The GCMC calculations were carried out using the sorption module of Cerius2 (Accelrys, San Diego) with the FF described in Ref. [15]. In order to obtain an accurate measure of H_2 loading, we used 1000 000 configurations to compute the average loading for each condition (pressure and temperature). To minimize undesirable boundary effects we used a finite three-dimensionally periodic cell containing four independent sheets each with 216 carbon atoms.
- [14] X. Xu and W. A. Goddard III, *Proc. Natl. Acad. Sci. U.S.A.* **101**, 2673 (2004).
- [15] G. H. Gao, T. Cagin, and W. A. Goddard III, *Phys. Rev. Lett.* **80**, 5556 (1998).
- [16] M. S. Dresselhaus *et al.*, *Science of Fullerenes and Carbon Nanotubes* (Academic Press, New York, 1996).
- [17] Q. Wang and J. K. Johnson, *J. Chem. Phys.* **110**, 577 (1999).
- [18] For these calculations we employed the CASTEP periodic QM software (from Accelrys) using the Perdew generalized gradient approximation II density functional combined with a plane-wave basis set. The geometries of Li-GIC or Li-PGS at various doping concentrations were fully optimized. We used a kinetic energy cutoff of 380 eV for the plane-wave basis set. We used the default convergence criteria which correspond to 0.0002 eV for the energy change per atom, 0.001 Å for the rms atomic displacement, and 0.05 eV/Å for the rms residual force.
- [19] R. Janot *et al.*, *Carbon* **39**, 1931 (2001).
- [20] T. Abe *et al.*, *Synth. Met.* **125**, 249 (2002); M. Inagaki *et al.*, *Carbon* **39**, 1083 (2001).
- [21] M. Barbatti *et al.*, *J. Chem. Phys.* **114**, 2213 (2001).